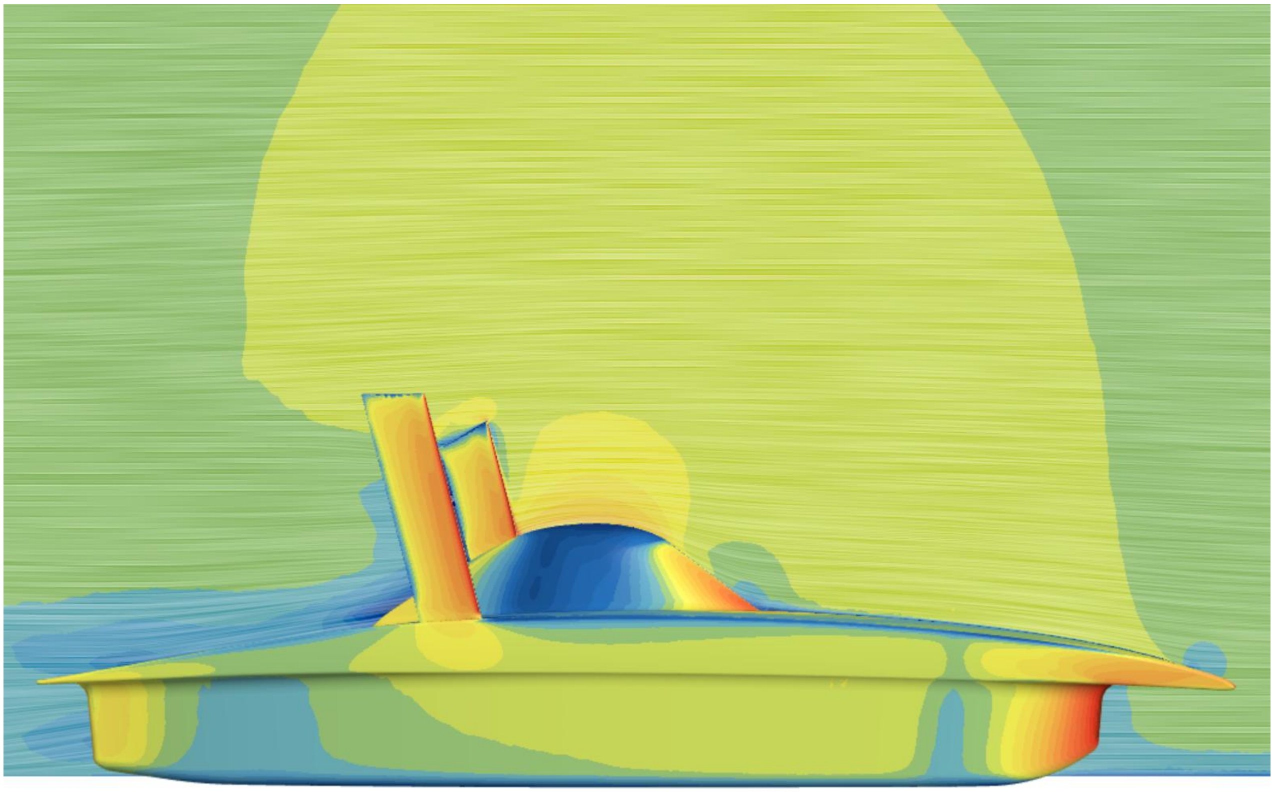

The Sailing Effect

Advantages and Disadvantages in Solar Car Racing

Author:

Benjamin Sheng

August 29th, 2026

Abstract

This project aimed to understand the effects of a retractable sail above the canopy of next generation solar cars. Top teams such as KU Leuven and Delft University solar car teams both have two retractable sails that come out from the canopy. In addition, Delft has a larger sail on the port side of the car that can be attached manually. This report attempts to analyze the performance of this sail and the aerodynamic effects being generated.

The base solar car model I used is a previous version of UBC Solar's final aeroshell which is a catamaran design with a front lip. The CAD phase involved adding a sail to the back half of the canopy in SolidWorks. This was followed by a CFD phase in Star-CCM where the model was placed in a virtual wind tunnel and simulated at 25m/s, 20 inflation layers, turbulence using a k-omega SST model, and the crosswind is 60 kilometers per hour at 30 degrees below the x-axis.

Table of Contents

1.0 – Introduction

The aerodynamic goal when developing a solar car is to be as close to a net zero lift and drag value without making the car dangerous. The cars need to glide through the air as efficiently as possible in order to utilize the least amount of battery power when driving. One particularly unfavorable condition for a solar car is heavy crosswinds. Crosswinds at 30 degrees increase our drag values by an average of 4 times based on UBC Solar CFD simulations. To counteract this, solar car teams have started to harness the crosswind by integrating retractable sail systems into their canopy. These sails can raise in the wind in order to generate thrust and help reduce that drag value.

Figure 1: Nuna 13S reveal

Top teams like TU Delft and KU Leuven both have two retractable sails coming out of the canopy tail. Furthermore, TU Delft has another sail on the portside of the car as well. On the surface this seems like an amazing idea. Harness the crosswind to generate thrust and push the car forwards. However, not every top team has these sails. Now many factors can contribute to this. Complexity, R&D time and cost are all potential reasons to not run a sail. Despite this, teams like Top Dutch, ETS, Sonnenwagen and Tokai are all top teams that do not have sails and are most likely not limited by resources. In addition, ETS was able to beat both TU Delft and KU Leuven at the Formula Sun Grand Prix this year without a sail. Understanding that many factors beyond aerodynamics go into winning a solar race, is there a trade-off to running a sail that can't be seen on the surface?

1.1 - How does a Sail Work?

The fastest way to sail isn't actually with the wind. When a sailboat sails with the wind, it is constrained by the speed of the wind itself. So if the wind is blowing at 10 kilometers per hour, then the boat can at most only match that speed. However, the hydrofoils that race in SailGP can achieve speeds over 100kph. How is this possible?

Figure 2: NorthStar Sail GP Team

Modern sails are like airfoils, generating high pressure on the windward side and lower pressure on the leeward side. This pressure difference generates lateral lift perpendicular to the direction of the wind hitting it, and that lift creates a vector component that acts as forward thrust. To balance the side force generated by the sail, the keel or foil of a sail (the carbon fin that sticks into the water in the photo above) generates a force that counteracts the sail's sideways push, keeping the boat from simply sliding sideways through the water. Despite its small size compared to the sail, the foil can match the sail's lateral force because water is roughly 800 times denser than air, so a much smaller surface area can generate an equivalent force. Rather than producing its own separate thrust, the foil's real contribution is twofold: by resisting leeway, it lets the sail's forward thrust actually translate into moving forwards instead of a sideways drift, and by lifting the hulls almost entirely clear of the water, it dramatically cuts the friction and drag from the waves that would otherwise limit the boat's top speed in the water. For these hydrofoil boats, it's a positive feedback cycle; the faster the boat goes, the greater the apparent wind hitting the sail becomes, generating more lift and letting the boat go even faster still. This lets modern foiling catamarans reach speeds in excess of 100 kph and sail 2 to 3 times faster than the true wind.

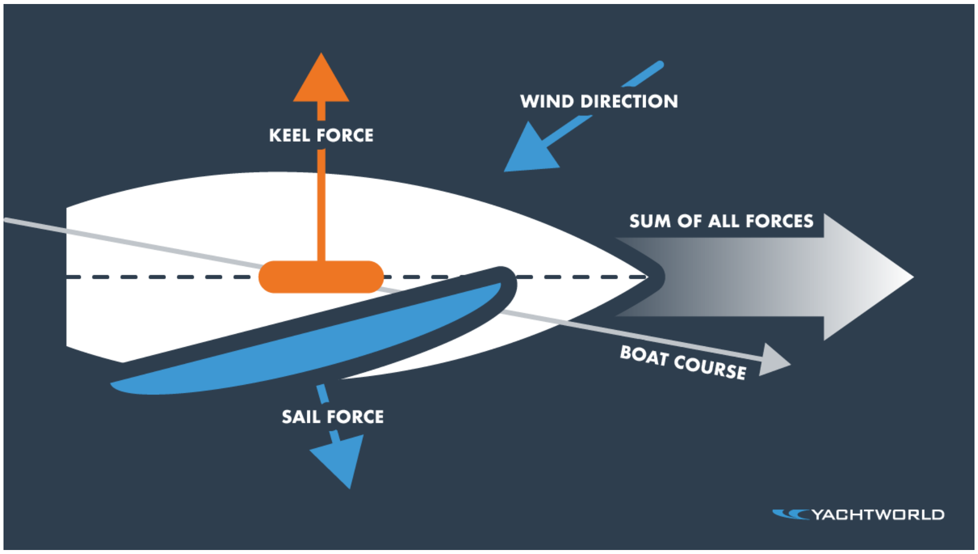

Figure 3: Diagram of how a sail works

This same concept can be applied to solar car racing. Next year, UBC Solar will be competing in the Formula Sun Grand Prix. This race will be located in Kansas. By looking up historical wind data around the track, I picked a middle number of 60kph at an angle of 30 degrees below the x-axis for my simulations. As you can see in the diagram below, the same thing will happen. The crosswind will create a lateral lift force perpendicular to the airflow, resulting in a thrust component propelling the car forwards. Furthermore, as the car drives faster, the apparent wind hitting the car will increase as well, replicating the positive feedback cycle present in hydrofoils. For all simulations, I've assumed an 80kph driving speed, resulting in an apparent wind of 135 kph at 12.8 degrees below the x-axis.

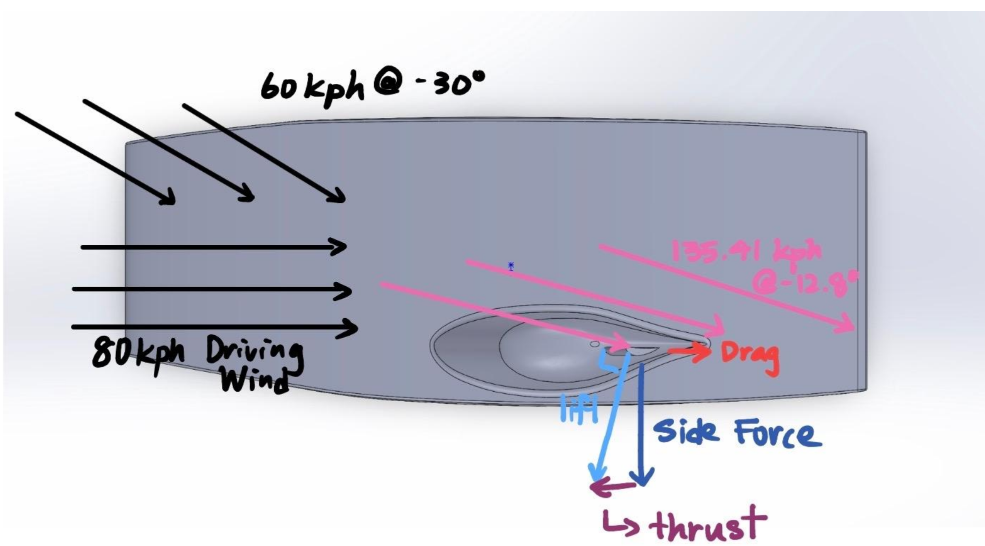

Figure 4: The sailing effect visualized on a Solar Car

2.0 – CAD Design

The base of this project was UBC Solar's EP9 Catamaran model (EP stands for Emilio Pous Avila the designer behind this model). This catamaran model is 1.88m by 4.88m. It consists of two hulls; the portside hull is thinner and where the battery sits, and the starboard hull (with the canopy) is where the driver sits. For the purpose of testing the sailing affect from placing airfoils vertically into the air, I simply added these airfoils into the existing model. No mechanisms or integration with other sub-systems in the car are included.

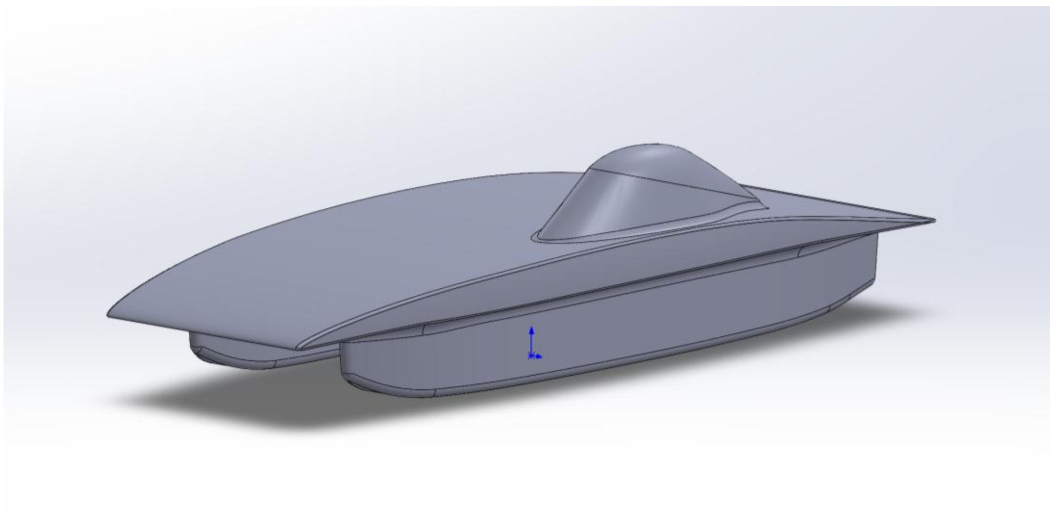

Figure 5: Isometric view of EP9

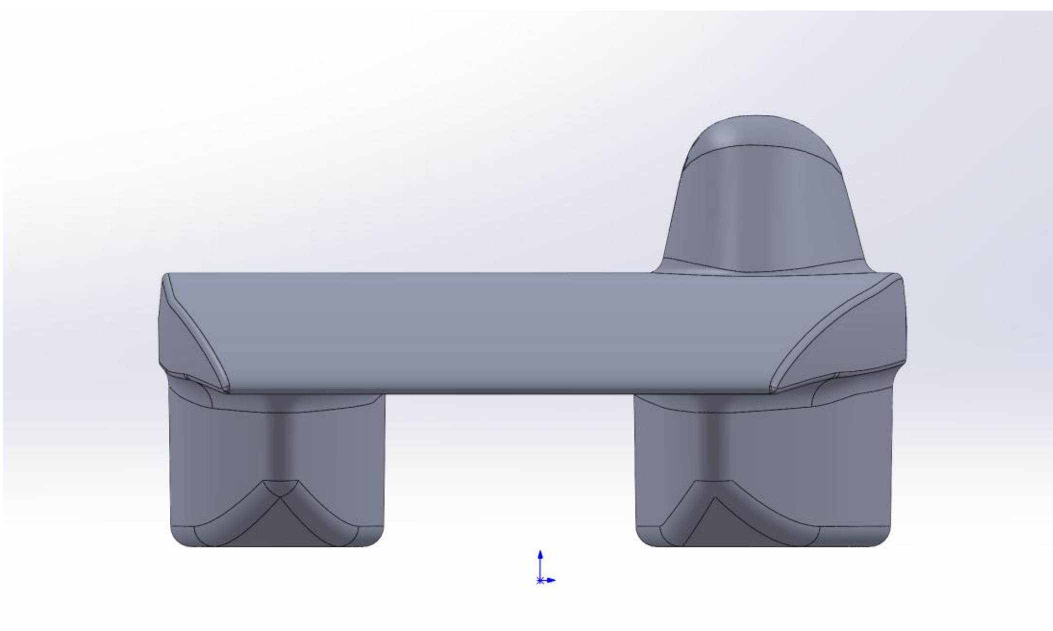

Figure 6: Front view of EP9

Taking inspiration from Nuna 13S, I visually tried to match the shape of the sail in JavaFoil, which is a software that can generate the co-ordinates for my airfoils and run simple analyses. Importing these into SolidWorks, I used two sketches at different planes to create a loft extrude solid body. Finally, to make sure that the sail could potentially sit flush within the canopy, I cut the top of the sail to the shape of the canopy's tail. This resulted in a sail that is 20 inches tall.

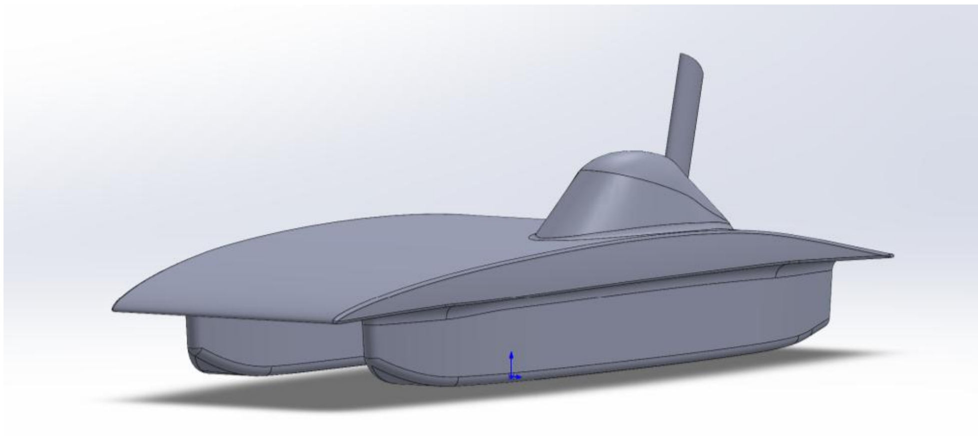

Figure 7: EP9 with canopy sail

Another distinctive aspect of Nuna 13S is their secondary sail on the port side of the car. I have also modeled this in the same way as the canopy side sail and will test it in CFD simulations. The model shown below has a 40in sail on the port side of the car.

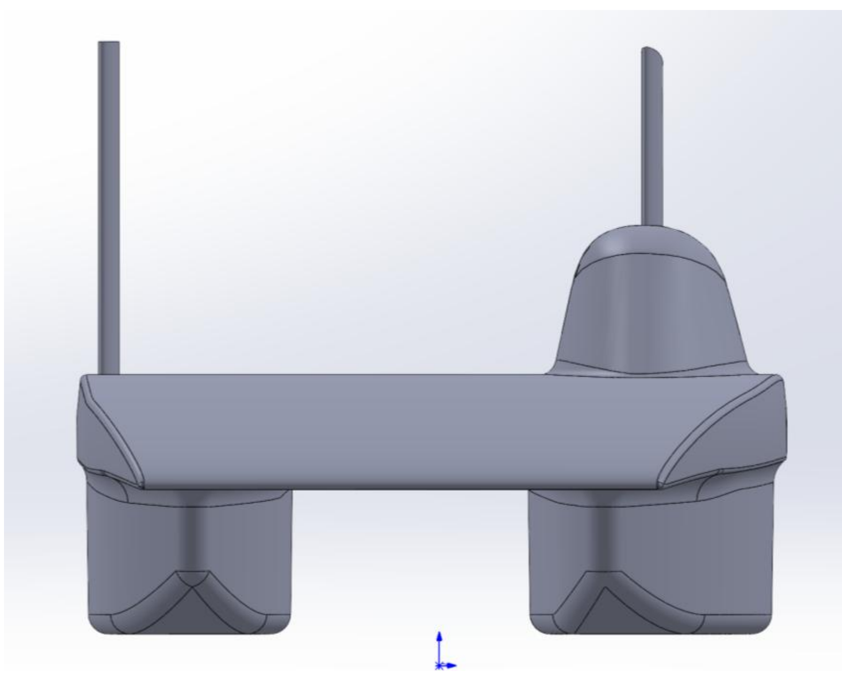

Figure 8: EP9 with two sails

3.0 – CFD Methodology

All CFD simulations were conducted on Simcenter StarCCM+. I did both 2D and 3D simulations to understand the effects of using vertical airfoils to sail.

3.1 – 2D Simulations

First, the airfoil that is to be tested is uploaded as a 3D CAD model. It is imported as a 3D curve and then extruded by 0.1m. Then, a domain is sketched around the airfoil on the xy plane. The domain size that was used is 20m behind the airfoil, 10m infront of the airfoil and 10m on either side. For a crosswind simulation, the windward side would stay at 10m and the windward side would extend to 20m. This is illustrated in figure 9. This domain is then extruded by 0.1m and boolean subtracted from the airfoil.

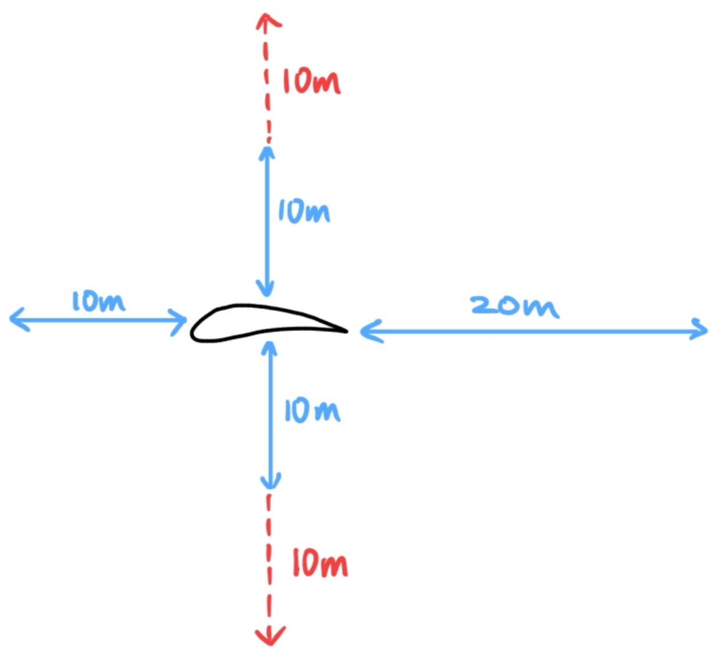

Figure 9: Domain Size for 2D Simulations

For the mesh, I used a polygonal mesher. Setting my base size to 0.1m and having the minimum surface size as 0.4% relative to the base size (4.0E-4m). The mesh also includes 30 prism layers at 10% relative to the base size (0.01m). In addition, a surface control was added for wake refinement. I set this wake refinement at 25% relative to the base size (0.025m) and at a growth rate at 1.5. This wake refinement was set at [1.0, 1.0, 0.0] or 45 degrees relative to the airfoil with a spread of 0.5 radian. This is to help with my workflow allowing me to test multiple crosswind angles in one direction using the same mesh. These settings resulted in the mesh shown in figure 10 below, consisting of 45,882 cells. It is important to note that this is not the finest mesh I could've run but it is what allowed me to run over 1000 iterations while still yielding good results within a decent time frame.

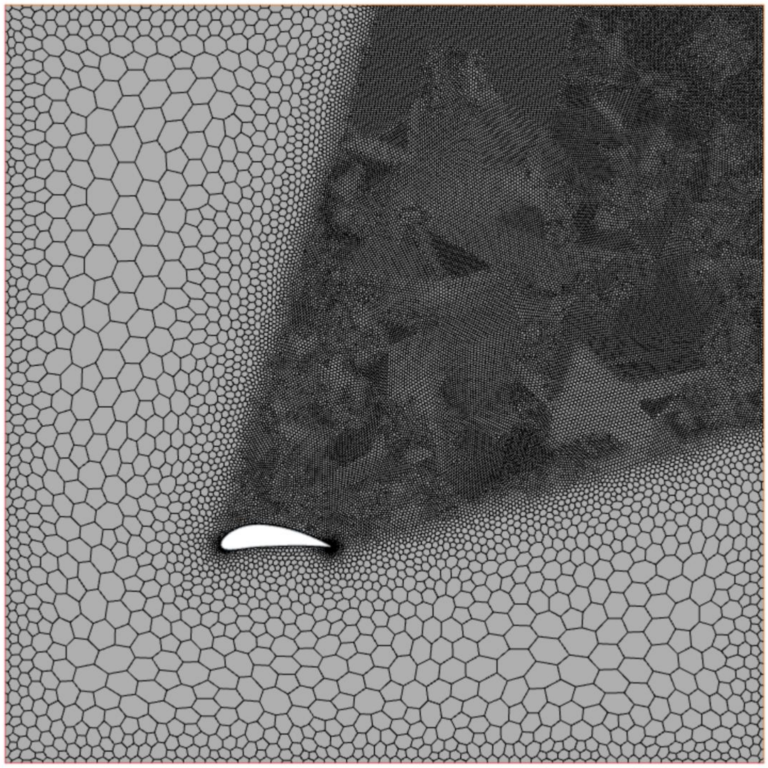

Figure 10: 2D Mesh on NACA10320 airfoil.

For the physics model the following were selected:

Material: Gas
Flow: Segregated Flow
Time: Steady
Equation of State: Constant Density
Viscous Regime: Turbulent
Reynolds Averaged Turbulence: K-Omega Turbulence
Initial Velocity: 30kph at 10, 20 and 30 degree angles

K-Omega Turbulence is chosen for its improved accuracy in resolving the near-wall boundary layer without relying on wall functions, which is important for this simulation since the flow is being evaluated at multiple angles (10°, 20°, and 30°). Segregated flow, constant density, and steady time are all appropriate selections given the nature of this simulation: at 30 kph (approximately 8.3 m/s), the flow is well within the incompressible regime (Mach number < 0.3), so a constant density assumption works, the segregated solver is suitable here because the flow does not involve strong pressure-velocity coupling or high-speed effects, allowing it to converge efficiently without the added memory overhead of a coupled solver, and a steady-state assumption is reasonable provided the flow remains largely attached or only mildly separated.

3.2 – 3D Simulations

For all 3D simulations, the CAD model of the car is imported as a 3D-CAD Model and then prepped for meshing. The sizing of my domain is shown in Figure 11. The domain is 12m long on the windward side and 25m long on the leeward side, as well as 5m in height. I've then created another block 12m by 12m around the car itself and towards the leeward side of the simulation. This is so I can set up a volumetric control and improve the mesh sizing in the wake of the car.

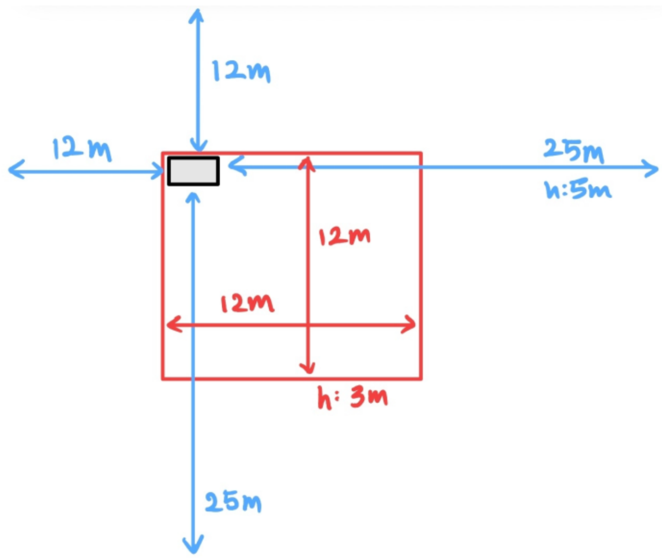

Figure 11: Domain size for crosswind simulations at -30 degrees

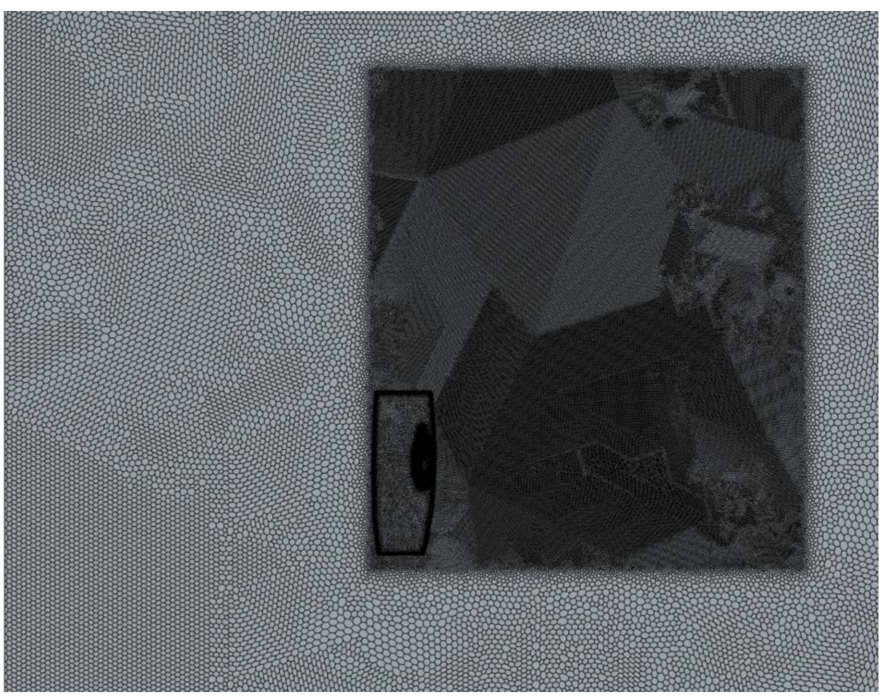

Figure 12: Section plane of mesh

For the mesh, I used a polyhedral mesher. Setting my base size to 0.1m and having the minimum surface size as 0.5% relative to the base size (0.001m). The mesh also includes 25 prism layers at 5% relative to the base (0.01m). For the volumetric control, I applied a custom size of 25% relative to the base (0.025m). The wake coming off the car at this speed is incredibly complex and this mesh refinement is crucial to getting good results. In the end, I was able to generate a mesh with around 14 million cells and 25 prism layers. The exact cell count would fluctuate depending on the model used.

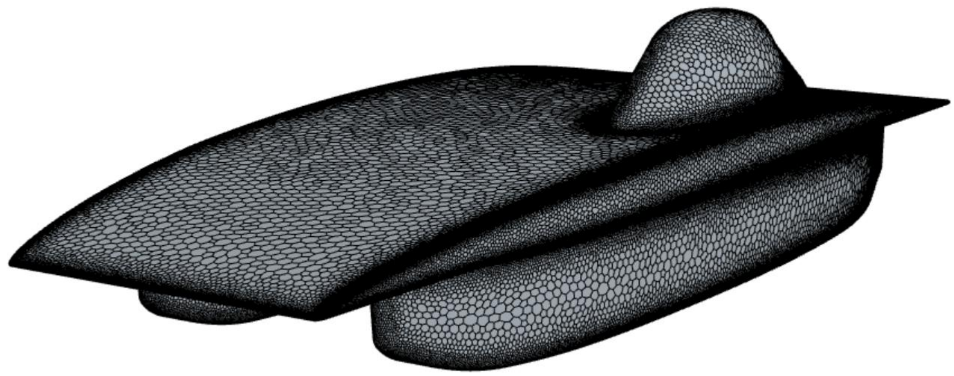

Figure 13: Car surface mesh

For the physics model the following were selected:

Material: Gas
Flow: Coupled Flow
Time: Steady
Equation of State: Constant Density
Viscous Regime: Turbulent
Reynolds Averaged Turbulence: K-Omega Turbulence
Initial Velocity: [30, 0, -131.9615] kph

Only difference here besides the initial velocity is the coupled flow. A segregated solver will solve each equation one at a time. Solving X-momentum and then Y-momentum and then Z. This is great for less complex simulations but when run with this velocity condition, the Sdr and Tke residuals would fluctuate like crazy and eventually the simulation would fail because the solver has diverged beyond the tolerance. The coupled solver will simultaneously solve these equations getting rid of the lag in the segregated flow approach. While more intensive on my computer, it was able to run the simulation without diverging.

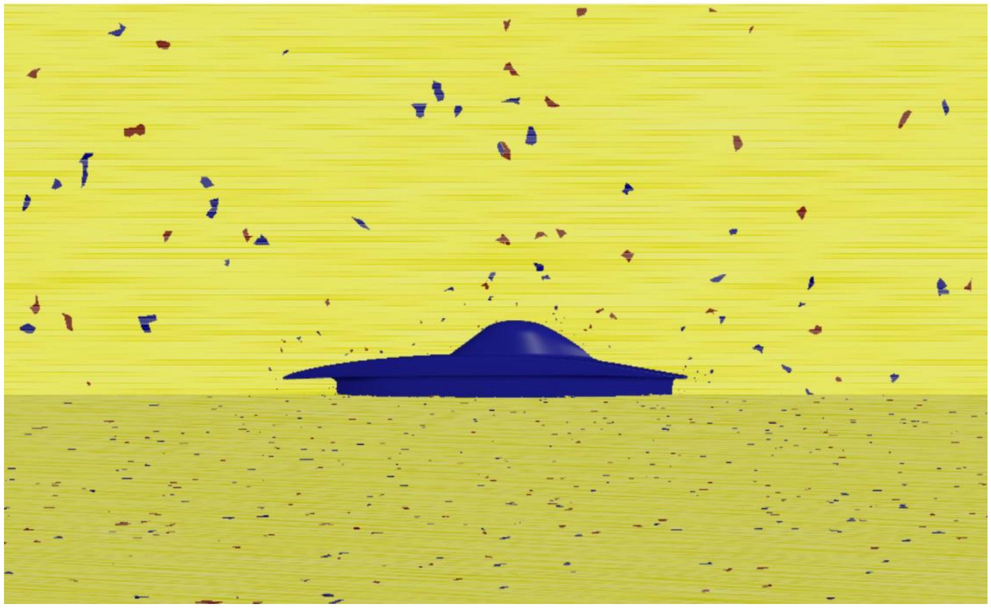

Figure 14: Initialized simulation

3.3 – Limitations

It is important to acknowledge that in the grand scheme of things these simulations may be heavily inaccurate. Without validating these CFD numbers with real world data, I can not confidently say that this is how the car will react under these circumstances in real life. Furthermore, there is a fine line between have a fine mesh and having the sim run on your laptop without taking ages. I could run meshes up to 20+ million cells on my laptop, however, generating the mesh and running the simulation would take days. Being limited by your hardware is the number one reason why these simulations may be inaccurate. A coarser mesh will lead to more inaccurate results, especially in this complex scenario where the car is traveling at 80kph while also experiencing a 60kph crosswind.

4.0 – Sail Analysis

I conducted five different simulations. 2D simulations on NACA10320 and Clark Y airfoils, as well as 3D simulations with the EP9 model, a singular canopy sail and then two sails on the car.

4.1 – NACA10320 Airfoil

Angle (Degrees)	Force	Pressure (N)	Shear (N)	Total (N)
10	Drag	-6.23	0.41	-5.82
	Lift	55.80	0.12	55.91
20	Drag	-13.43	0.33	-13.09
	Lift	71.50	0.17	71.72
30	Drag	-17.60	0.23	-17.38
	Lift	78.34	0.161	78.51

Table 1: NACA10320 2D simulation numbers

Across the three angles tested, the NACA10320 airfoil shows a clear trend: both lift and drag magnitude increase as angle of attack increases from 10° to 30°. Lift rises from 55.91 N at 10° to 71.72 N at 20° and 78.51 N at 30°, while drag grows in magnitude from -5.82 N to -13.09 N to -17.38 N over the same range. Notably, the increase in lift is not linear. The jump from 10° to 20° adds nearly 16 N, while the jump from 20° to 30° only adds about 6.8 N. This diminishing rate of lift increase suggests the airfoil is approaching the upper portion of its lift curve, where the rate of lift generation per additional degree of angle begins to taper off as the airfoil nears stall.

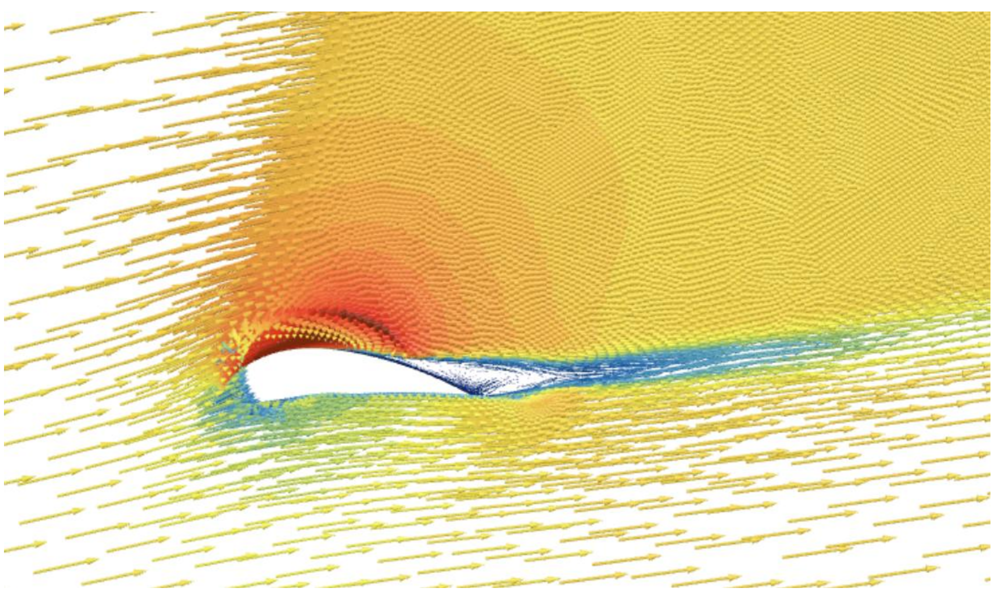

Figure 15: NACA10320 vector field

The vector plot for the NACA10320 case shows a largely attached flow field, with a well-defined thin wake trailing off the back of the airfoil and only a small region of recirculation near the leading edge on the suction side. This is consistent with the force data: attached flow over most of the chord allows the airfoil to keep generating strong lift gains as angle increases, but the presence of that early separation bubble hints at why the lift-curve slope is already beginning to flatten by 20-30°.

4.2 – Clark Y Airfoil

Angle (Degrees)	Force	Pressure (N)	Shear (N)	Total (N)
10	Drag	-8.25	0.47	-7.77
	Lift	55.51	0.07	55.58
20	Drag	-16.50	0.26	-16.30
	Lift	64.60	0.09	64.77
30	Drag	-2.19	0.29	-1.90
	Lift	66.70	0.006	66.73

Table 2: Clark Y 2D simulation numbers

The Clark Y airfoil follows a broadly similar pattern to the NACA10320 at lower angles, but the numbers reveal a more abrupt transition between 20° and 30°. Lift increases from 55.58 N at 10° to 64.77 N at 20°, a gain comparable to the NACA case, but only rises marginally further to 66.73 N at 30° which is a much smaller increment than what was seen for the NACA10320 over the same range. Drag magnitude grows from -7.77 N at 10° to -16.30 N at 20°, roughly in line with expectations, but then drops sharply to just -1.90 N at 30°, despite the higher angle of attack. As with the NACA airfoil, shear forces remain small relative to pressure forces throughout, confirming that pressure distribution is again the dominant contributor to both lift and drag.

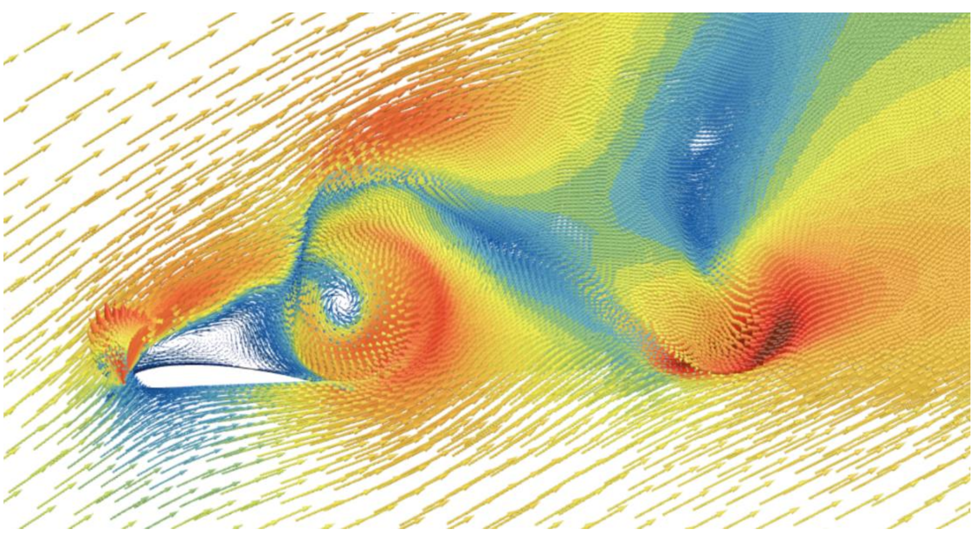

Figure 16: Clark Y vector field

This sharp drop in drag magnitude alongside the near-plateau in lift between 20° and 30° is a strong indicator that the Clark Y airfoil has crossed into stall by the time it reaches 30°. Once an airfoil stalls, the large low-pressure suction peak near the leading edge that drives both high lift and high pressure drag collapses as the flow separates over most of the upper surface, which explains why drag magnitude falls even as angle of attack increases further. This behavior is more abrupt than what the NACA10320 showed over the same angle range, which is consistent with the Clark Y's flatter-bottomed, more cambered geometry. This shape tends to produce strong lift and pressure drag increases at moderate angles but can stall more suddenly once the adverse pressure gradient overwhelms the boundary layer. Compared side-by-side, the two airfoils highlight a useful contrast for this study: the NACA10320 is still gaining lift steadily through 30°, while the Clark Y appears to have already passed its peak lift-to-drag efficiency somewhere between 20° and 30°.

The NACA10320 outperforms the Clark Y across the board, generating more lift at every angle tested (78.51 N vs. 66.73 N at 30°) and a better lift-to-drag ratio through 10° and 20° (roughly 9.6 and 5.5, versus 7.2 and 4.0 for the Clark Y). More importantly, its lift curve stays consistent and keeps climbing all the way to 30°, while the Clark Y's numbers suggest it stalls somewhere between 20° and 30°, where lift plateaus and drag collapses and a deceptively high L/D ratio at that point that actually reflects lost lift-generating capability rather than genuine efficiency. Since this analysis spans 10° to 30°, the NACA10320's ability to keep producing strong, predictable lift across that full range makes it the more reliable and higher-performing airfoil of the two.

4.3 – Control: EP9 Catamaran

Component	Force	Pressure (N)	Shear (N)	Total (N)
Car	Drag	4.50	64.04	68.54
	Lift	-308.25	-0.44	-308.69

Table 3: EP9 3D simulation numbers

The EP9 catamaran control case shows drag dominated by shear rather than pressure, with 64.04 N of the 68.54 N total coming from skin friction and only 4.50 N from pressure. This suggests well-attached flow over most of the car body with minimal drag. Lift, on the other hand, is almost entirely pressure-driven, with -308.25 N of the -308.69 N total coming from pressure and a negligible shear contribution. The large negative lift value indicates significant downforce being generated due to the large tunnel section between the two hulls. This model serves as a useful reference point for evaluating how the addition of sails in the later sections changes both the drag and downforce produced by the car

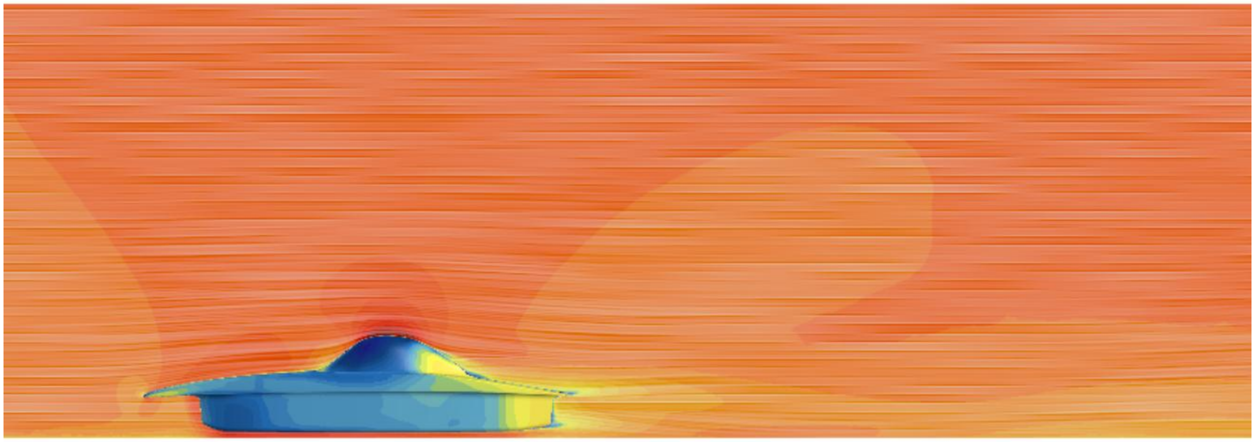

Figure 17: Side velocity vector flow field

This side view in figure 17 shows the flow accelerating as it passes over the raised canopy section of the car body, visible in the compressed, tightly-packed flow lines directly above the hump. Just downstream of this high point, the flow separates off the rear of the body, generating a visible recirculation region in the wake, shown by the faded, disturbed pattern trailing off to the upper right. This is a typical result for a bluff, rounded body shape. The flow can't stay attached all the way around the curvature, so it separates near the rear, creating a low-pressure wake that contributes to the car's overall drag.

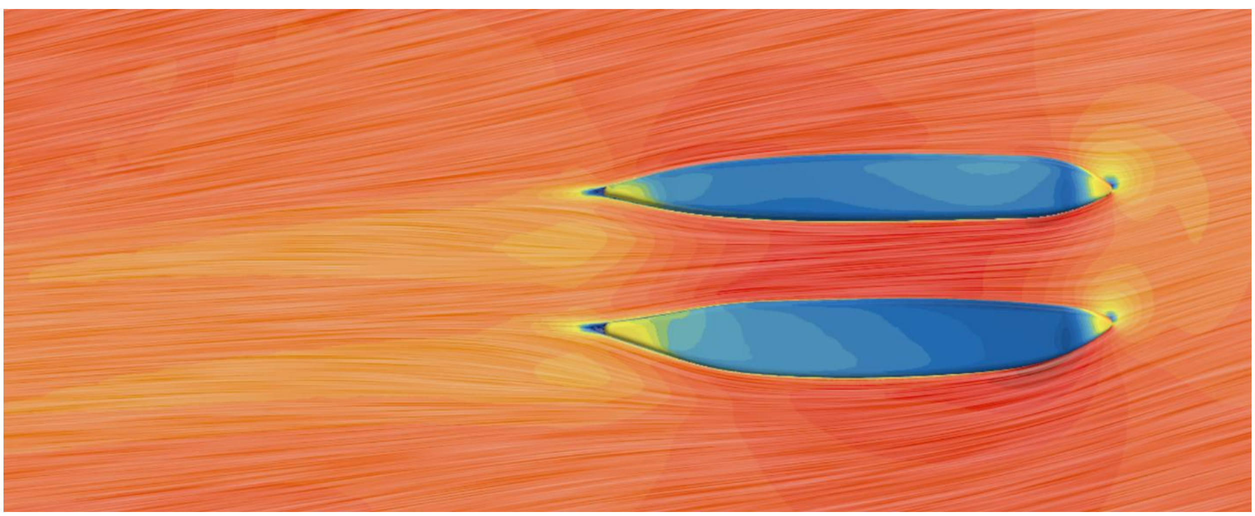

Figure 18: Underside velocity vector flow field

This bottom-side view in figure 18 shows the flow passing around the car's twin-body layout, with the flow accelerating through the narrow channel between the two hulls where the streamlines compress together. At the trailing tips of each hull, a distinct area of low pressure forms where the flow separates and rolls off into a turbulent wake, and because the two hulls sit close together, their individual wakes are close enough to interact rather than developing independently.

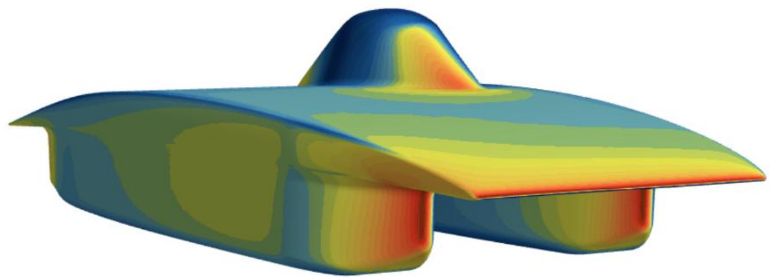

Figure 19: EP9 pressure gradient

The pressure contour in figure 19 shows a tightly concentrated gradient near the leading edge of the surface, with the strongest pressure change confined to a small stagnation-like region before spreading out into a much more gradual, uniform gradient across the surrounding far-field. This kind of sharp, localized peak at the leading edge followed by a outward pressure distribution is typical of a lifting surface where the flow first meets the body directly, generating a strong local pressure differential before the flow settles into the broader domain. It's this concentrated leading-edge pressure difference that is largely responsible for the strong pressure-driven downforce seen in the force table above.

4.4 – Canopy Side Sail

Component	Force	Pressure (N)	Shear (N)	Total (N)
Car	Drag	-9.27	64.09	54.82
	Lift	-485.09	-0.56	-485.66
Canopy Side Sail	Drag	-18.02	0.77	-17.25
	Lift	154.94	0.29	155.24

Table 4: EP9+Canopy sail numbers

With the canopy side sail added, the car body shows a total drag of 54.82 N, dominated by shear (64.09 N) rather than pressure (-9.27 N), and a total lift of -485.66 N that's almost entirely pressure-driven (-485.09 N), indicating strong downforce. The canopy side sail itself contributes -17.25 N of drag, again pressure-dominated (-18.02 N pressure vs. 0.77 N shear), and generates 155.24 N of lift, with pressure accounting for nearly all of it (154.94 N).

Lift to Thrust Conversion:
Canopy Side Sail: tan(12.8) = opposite/155.24N 155.24*tan(12.8) = Thrust Thrust = 35.27N

Table 5: EP9+Canopy sail lift to thrust conversion

35.27	+ 17.25	– 54.82
Canopy Side Thrust	Canopy Side Drag	Car Drag
Overall Drag Number: 2.3N of Drag		

Table 6: EP9+Canopy sail final drag numbers

Using the sail's 155.24 N of lift and a resolved angle of 12.8°, that lift converts to 35.27 N of forward thrust via tan(12.8°) = thrust/155.24. Combining this thrust and the sail's drag, which is only thrust (17.25 N), against the car body's drag (54.82 N) leaves a net system drag of just 2.3 N, meaning the thrust generated by the sail nearly cancels out the combined drag of the car and sail entirely.

Figure 20: Left side velocity vector flow field

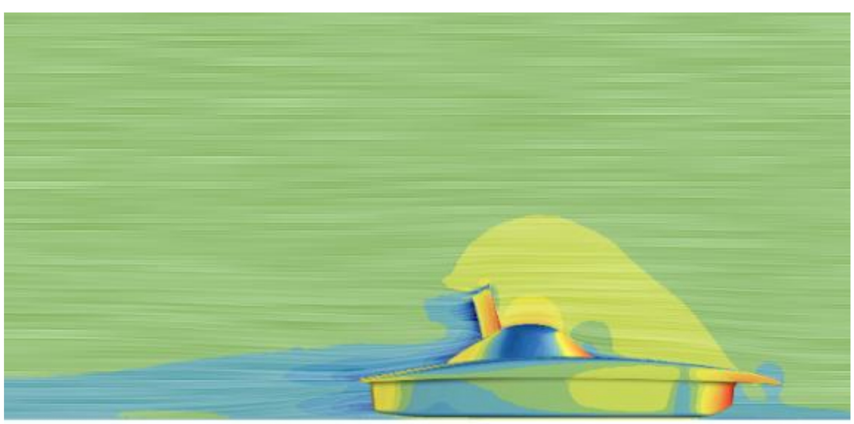

Figure 21: Right side velocity vector flow field

The close up in figure 22, isolates the flow immediately around the canopy side sail, showing a strong, elongated low-velocity wake trailing directly off the sail, visible as the dark blue streak extending through the frame. A small red high-velocity/pressure spot sits right at the base of the sail, likely marking where the flow first meets the surface before rapidly decelerating and separating into the wake downstream. This concentrated wake is consistent with the sail acting as an effective lifting surface, generating a strong pressure differential that sheds a well-defined structure behind it.

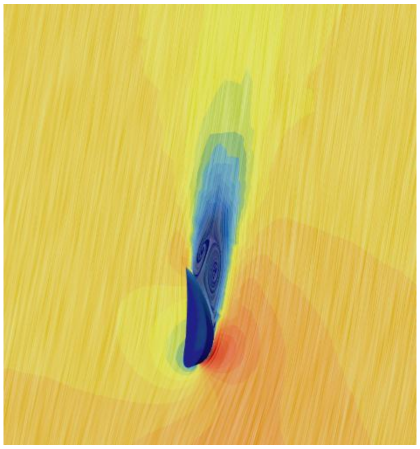

Figure 22: Sail velocity vector flow field

The contour plot in figure 23 shows the pressure distribution across the EP9 body with the canopy sail installed, with a concentrated low-pressure region (blue) directly around the canopy hump surrounded by a warmer ring where the flow accelerates most sharply. Moving toward the rear hulls, the surface shifts into yellow and orange tones, suggesting the flow has decelerated and pressure has recovered somewhat after passing over the canopy. This shows the sail's influence extends across the whole body's pressure field rather than staying localized to the sail itself, which helps explain why the car component alone shows such a large downforce figure in the numbers above.

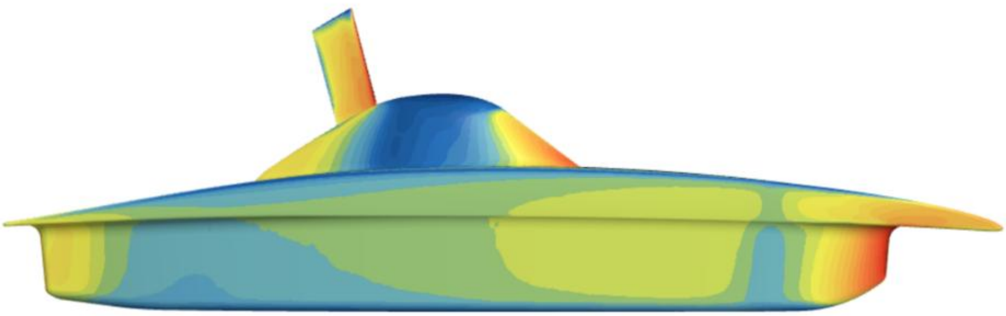

Figure 23: EP9+sail pressure gradient

4.5 – Two Sails

Component	Force	Pressure (N)	Shear (N)	Total (N)
Car	Drag	-5.53	64.12.	58.59
	Lift	-323.79	-0.79	-324.58
Battery Side Sail	Drag	-36.24	1.39	-34.85
	Lift	304.44	0.57	305.02
Canopy Side Sail	Drag	-17.10	0.80	-16.29
	Lift	156.90	0.29	157.2

Table 7: EP9+Two sails 3D simulation numbers

With two sails now installed, the car body shows a total drag of 58.59 N, again dominated by shear (64.12 N) over pressure (-5.53 N), and a total lift of -324.58 N driven almost entirely by pressure (-323.79 N). The battery side sail contributes -34.85 N of drag (-36.24 N pressure) and 305.02 N of lift (304.44 N pressure), while the canopy side sail adds -16.29 N of drag (-17.10 N pressure) and 157.2 N of lift (156.90 N pressure). Both sails again derive essentially all their force from pressure rather than shear, consistent with their role as thin lifting surfaces, with the battery side sail producing nearly twice the lift of the canopy side sail (it's double the size so this makes sense).

Lift to Thrust Conversion:	
Battery Side Sail: tan(12.8) = opposite/305.02N 305.02N*tan(12.8) = Thrust Thrust = 69.30N	Canopy Side Sail: tan(12.8) = opposite/157.2N 157.2N*tan(12.8) = Thrust Thrust = 35.71N

Table 8: EP9+two sails lift to thrust conversion

69.30 +	34.85 +	35.71 +	16.29 –	58.59
Battery Side Thrust	Battery Side Drag	Canopy Side Thrust	Canopy Side Drag	Car Drag
Overall Drag Number: 97.56N of Thrust				

Table 9: EP9+two sails overall drag calculation

Using each sail's lift and the same 12.8° angle, the battery side sail's 305.02 N of lift converts to 69.30 N of thrust, and the canopy side sail's 157.2 N converts to 35.71 N of thrust. Combining both thrust and drag contributions: 69.30 + 34.85 + 35.71 + 16.29 − 58.59 yields a net positive 97.56 N of thrust, meaning with both sails installed, the combined thrust now exceeds the total drag from the car and sails, producing a net forward driving force rather than a net drag

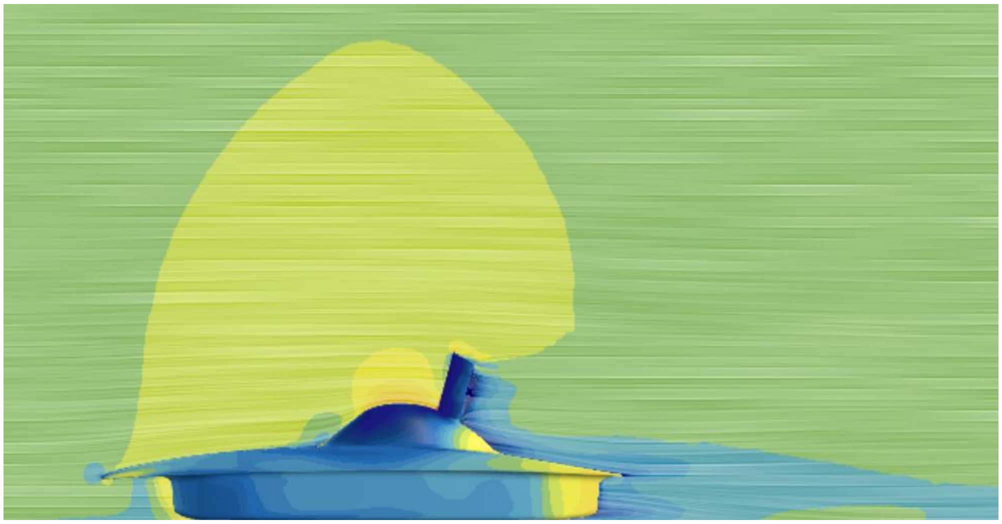

Figure 24: Canopy side velocity vector flow field

These two side view plots again show the same flow field around the EP9 body from two different sides, now with both sails installed, and the pattern is consistent between them. The flow accelerates sharply over the canopy hump, forming the same wide high-velocity band seen in the single-sail case, while a lower-velocity wake region develops just behind and around the base of the two sail structures. The agreement between the two views again confirms the flow is behaving symmetrically about the car's centerline, even with the second sail added.

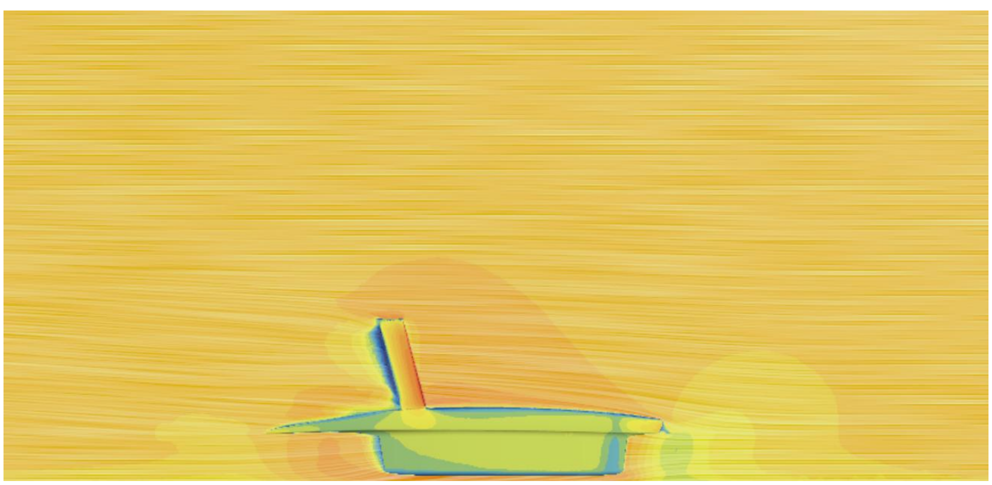

Figure 25: Battery side velocity vector flow field

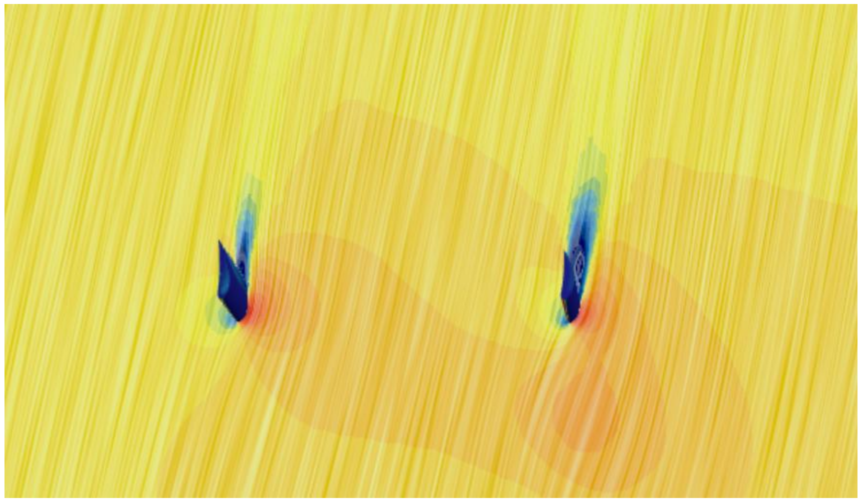

Figure 26: Two sail velocity vector flow field

Figure 26 shows two separate wake structures, one trailing off each sail, rather than the single wake seen in the canopy-only configuration. Both wakes look similar in shape and strength, each with a distinct low-velocity streak and a small high-velocity/pressure spot at its base, suggesting the two sails are behaving similarly and largely independently rather than interfering heavily with one another's flow field. This supports the numbers above, the two-sail setup is achieving close to double the lifting effect without a major wake interaction penalty between the sails.

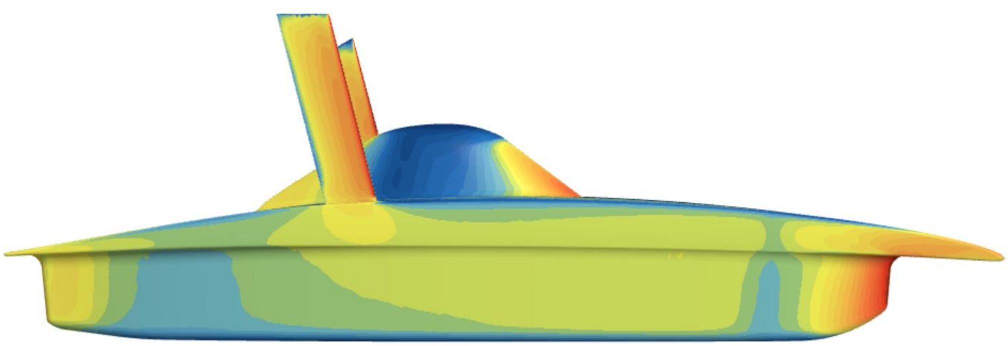

Figure 27: EP9+two sails pressure gradient

This contour plot in figure 27 shows the pressure distribution across the EP9 body with both sails installed, now showing two angled sail structures rising from the canopy area instead of one. The pressure pattern around the base of each sail looks similar to the single-sail case, with a concentrated low-pressure region transitioning into warmer tones across the rest of the body toward the rear pontoons. The similarity between the one- and two-sail pressure patterns suggests the second sail isn't meaningfully disrupting the pressure field established by the first, which lines up with both sails still producing strong, largely independent lift and thrust contributions.

5.0 – Conclusion

In conclusion, the results of this study make a strong case that the sailing effect is worth pursuing further. The baseline EP9 catamaran control case showed the car body alone producing 68.54 N of drag, and adding a single canopy sail nearly cancelled that out entirely, leaving a net system drag of just 2.3 N once the sail's thrust component was accounted for. With two sails installed, the results went a step further: the combined thrust from both sails exceeded the total drag of the car and sails, producing a net positive 97.56 N of forward-driving force rather than a net drag. Going from a car that has to fight through 60+ N of drag to one that gains a net aerodynamic push under the same crosswind condition is the kind of performance gap that's worth chasing.

That said, these results need to be read with the limitations of this study in mind. All of these numbers come from a single crosswind condition (60 kph at 30 degrees), a single driving speed (80 kph), and steady-state CFD simulations that haven't been validated against real-world wind tunnel or on-track data, so there's no way to confirm how closely these numbers reflect actual performance. Real life crosswinds do not act as simply as we think, and broader race strategy considerations must be taken into account. Mesh resolution was also constrained by available hardware. My 3D simulations topped out at around 14 million cells, and finer meshes that could better resolve the highly complex wake behind the car simply weren't feasible to run in a reasonable timeframe. Because of this, the absolute force values reported here should be treated as directional estimates of the sailing effect's potential rather than precise predictions of on-track performance.

Even accounting for that uncertainty, the scale of the effect seen here, moving from significant net drag to net thrust, is large enough that it's unlikely to be purely a modeling artifact. Given that some of the top solar car teams in the world have already reached the same conclusion independently, and that this study reinforces it with an actual net-positive thrust result for the two-sail configuration, I believe the sailing effect is an important project for UBC Solar to continue developing. The next steps should focus on closing the gaps identified above: validating these results with a physical prototype or wind tunnel testing, running higher-fidelity simulations across a broader range of crosswind angles and speeds, and evaluating the practical cost of implementation, including the retraction mechanism, added structural weight, and integration with the rest of the car, since those factors, not aerodynamics alone, will ultimately determine whether a sail is worth carrying onto the track.

6.0 – Appendix

6.1 – More CFD Photos

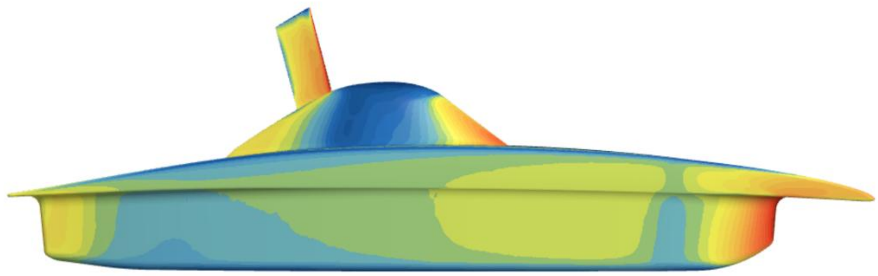

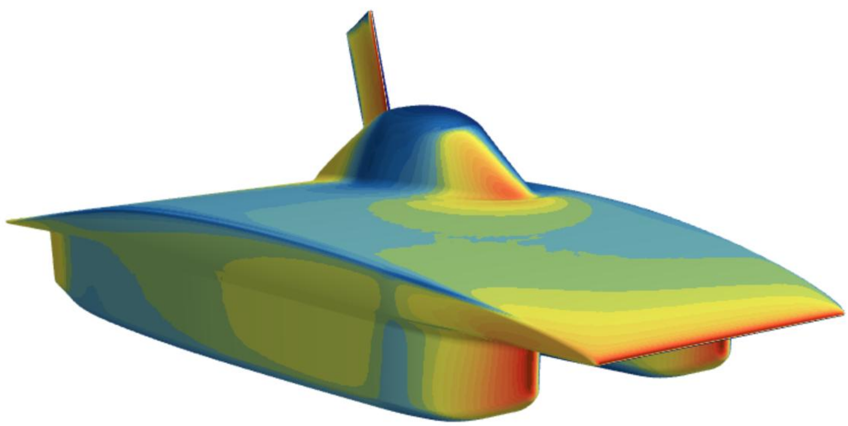

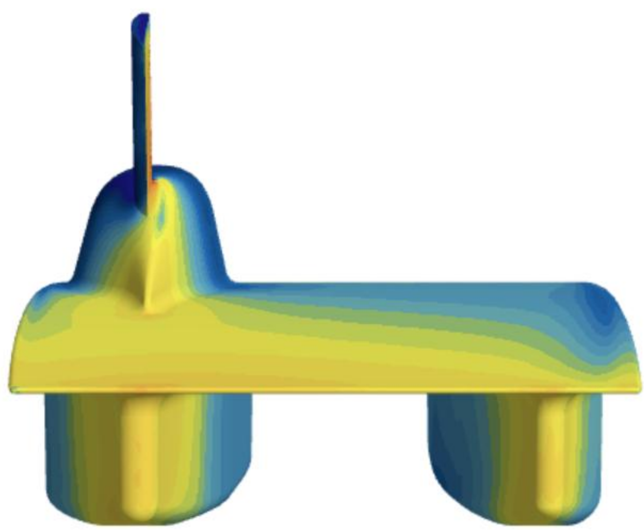

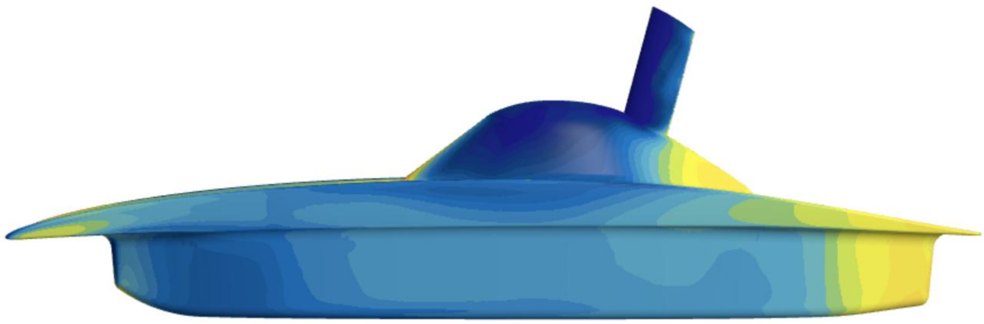

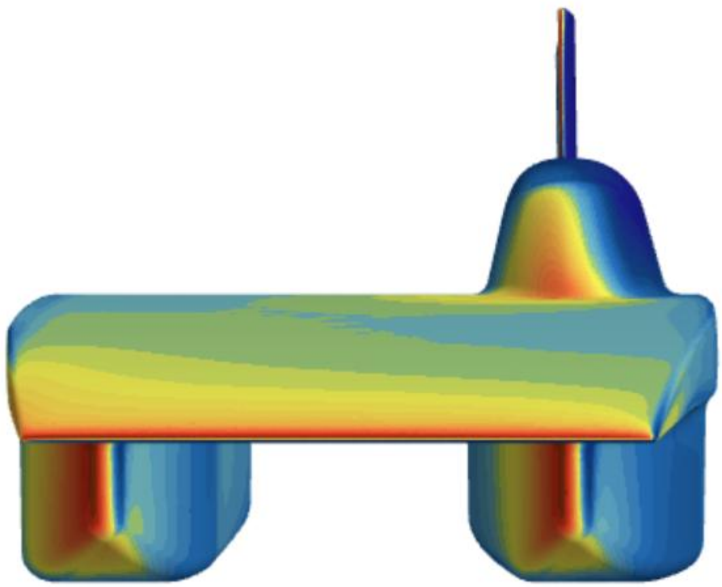

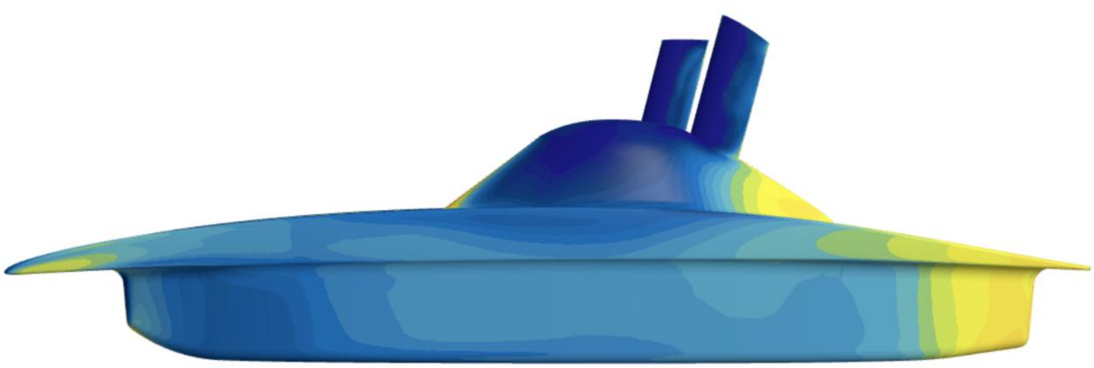

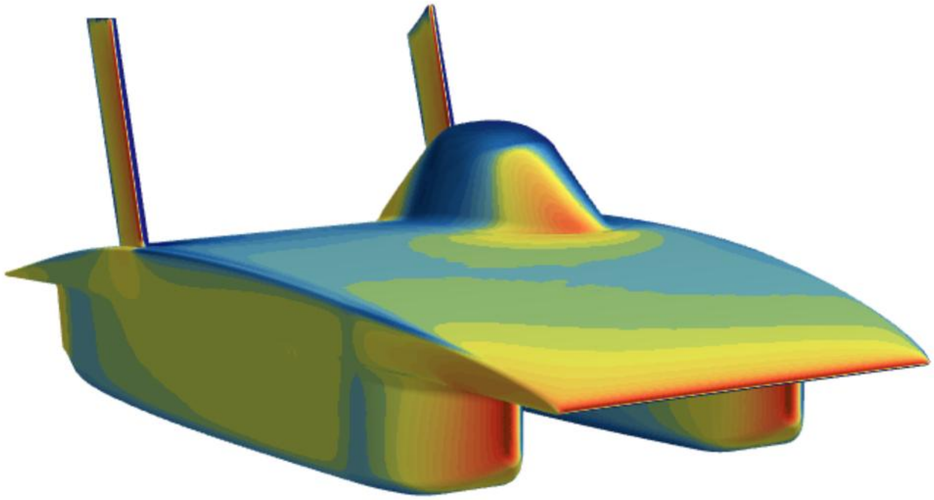

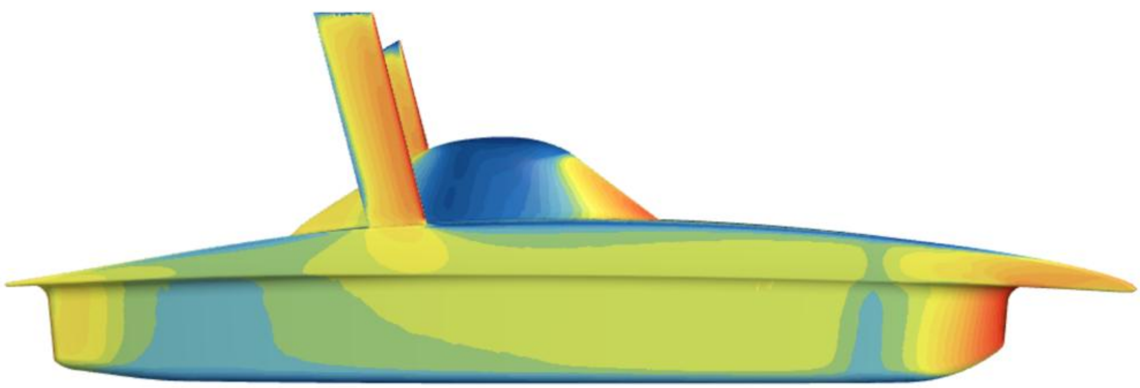

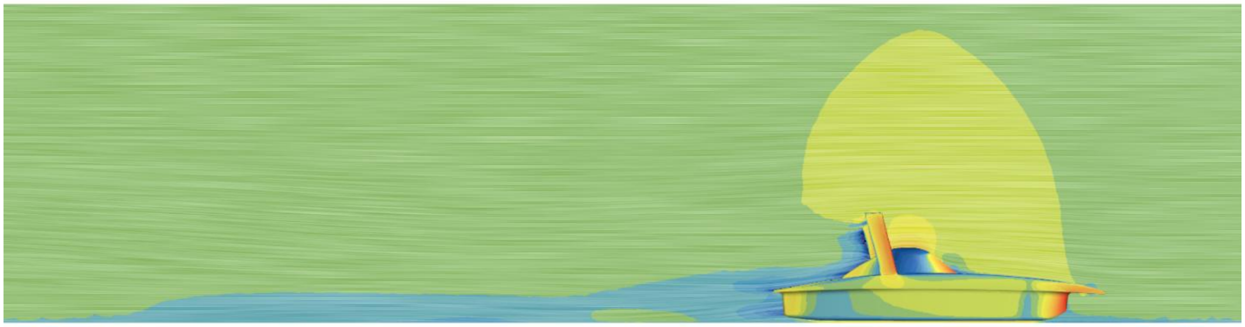

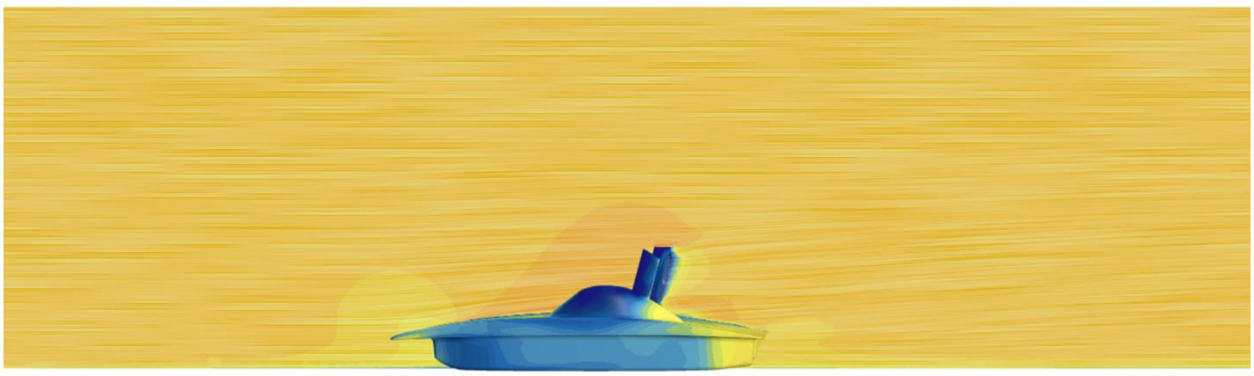

6.2 – Figures List

6.3 – Tables List